miR-130A as a Diagnostic Marker to Differentiate Malignant Mesothelioma From Lung Adenocarcinoma in Pleural Effusion Cytology

Rocco Cappellesso, MD [1]; Marco Galasso, PhD[2]; Lorenzo Nicolè, MD[1]; Paolo Dabrilli, BD[1]; Stefano Volinia, PhD[2]; and Ambrogio Fassina, MD[1]

BACKGROUND: Malignant pleural mesothelioma is a rare tumor with a dismal prognosis, usually presenting with recurrent effusions. However, the majority of malignant pleural effusions are due to lung adenocarcinoma (AdC). The distinction between these tumors has considerable therapeutic and medicolegal implications and can be very challenging both histologically and cytologically. Appropriate immunohistochemistry (IHC) is required to support the diagnosis. MicroRNA (miRNA) expression analysis could be a viable diagnostic tool for distinguishing between these tumors. The purpose of the current study was to assess the reliability of miRNAs as diagnostic markers to differentiate epithelioid malignant mesothelioma (MM) from lung AdC. **METHODS:** Bioinformatic analysis of publicly searchable data sets regarding miRNA expression profiling was performed to select the most significant differentially expressed miRNAs. These were analyzed by quantitative polymerase chain reaction on histologic (41 MM cases and 40 lung AdC cases) and cytological (26 MM cases and 27 lung AdC cases) specimens and the diagnostic performances were assessed. **RESULTS:** miR-130a, miR-193a, miR-675, miR-141, miR-205, and miR-375 were found to be the best distinguishing markers. Of these, only miR-130a was significantly overexpressed in MM compared with lung AdC (P =.029 in histologic and P =.014 in cytological samples). miR-130a demonstrated a sensitivity of 77%, a specificity of 67%, a positive predictive value of 69%, a negative predictive value of 75%, and an accuracy of 72% in identifying MM. **CONCLUSIONS:** The diagnostic performances of miR-130a expression analysis and IHC appear to be similar. miR-130a quantification could be used reliably as second-level diagnostic tool to differentiate MM from lung AdC in pleural effusion cytology, mainly in those cases with ambiguous or negative IHC. Further validation is needed. ***Cancer Cytopathol* 2017;125:635-43**. © *2017 American Cancer Society*.

KEY WORDS: lung adenocarcinoma; malignant mesothelioma; miR-130a; pleural effusion.

INTRODUCTION

Malignant mesothelioma (MM) is a tumor with a poor prognosis that arises from the mesothelial cells lining the serosal surfaces.[1] The global incidence of MM is rising dramatically, and is expected to hit its peak in Europe within the next decade.[2] MM typically is related to the long-term inhalation of asbestos fibers and the pleura is the most commonly affected site. According to the World Health Organization classification, 3 subtypes of MM are recognized: epithelioid MM (resembling an adenocarcinoma [AdC]), sarcomatoid MM (composed of spindle cells), and biphasic MM (a mix of the other 2 subtypes).[3]

International Mesothelioma Interest Group (IMIG) guidelines state that the diagnosis of MM always should be based on the results obtained from an adequate biopsy within the context of proper clinical, radiologic,

Corresponding author: Ambrogio Fassina, MD, Surgical Pathology and Cytopathology Unit, Department of Medicine, University of Padua, Via Gabelli, 61, 35121 Padua, Italy; Fax: (011) 39 049 8273782; ambrogio.fassina@unipd.it

[1]Surgical Pathology and Cytopathology Unit, Department of Medicine, University of Padua, Padua, Italy; [2]Laboratorio per le Tecnologie delle Terapie Avanzate, Department of Morphology, Surgery, and Experimental Medicine, University of Ferrara, Ferrara, Italy.

Received: November 14, 2016; **Revised:** March 3, 2017; **Accepted:** March 20, 2017

Published online April 27, 2017 in Wiley Online Library (wileyonlinelibrary.com)

DOI: 10.1002/cncy.21869, wileyonlinelibrary.com

and surgical findings.[4] Moreover, the histologic diagnosis of MM is mandatorily based not only on appropriate morphology, but also on adequate immunohistochemistry (IHC) due to the overlapping features of MM with several carcinomas, mainly peripherally located lung AdC involving the pleura.[4,5] Patients with pleural MM usually present with advanced stage disease and recurrent pleural effusions (PE), and the cytological examination of the exfoliated cells (almost exclusively of epithelioid type) is usually the initial, and often exclusive, approach to the diagnosis.[6] The reported sensitivity of the cytological diagnosis of MM based on morphology alone is historically low, and this accounts for its exclusion from the IMIG guidelines.[4] However, accumulating evidence has indicated that MM cytology supported by ancillary techniques is as reliable as histology, although the sensitivity of cytology remains somewhat lower.[7] Also in this setting, the application of IHC to cell block sections is compulsory because it greatly enhances the diagnostic performance of cytology and enables the differentiation of MM from other PE-associated carcinomas, including lung AdC, with all the subsequent therapeutic and medicolegal implications.[7]

A plethora of IHC markers have been proposed for this purpose, and these markers usually are divided into "mesothelial" (eg, cytokeratin 5/6, calretinin, Hector Battifora mesothelial epitope-1 (HBME-1), thrombomodulin, Wilms tumor 1 [WT1], mesothelin, D2-40, vimentin, H-caldesmon, and CD90 [Thy-1])[8-12] and "epithelial" (eg, thyroid transcription factor 1 [TTF-1]; napsin A; carcinoembryonic antigen; Ber-EP4; MOC-31; B72.3; CD15; Lewis y; claudin-4; and mucin 4, cell surface associated [MUC4]) markers.[11-17] However, when taken alone, none of these antibodies was found to provide the required sensitivity and specificity to distinguish MM from lung AdC. For this reason, IMIG guidelines currently indicate the use of an antibody panel including at least 2 mesothelial and 2 epithelial markers with a sensitivity or specificity >80%.[4]

MicroRNAs (miRNAs) are a well-known class of regulatory, short, noncoding RNA molecules that often have been reported as being tumor specific.[18] Moreover, miRNA expression analysis is feasible in cytological specimens and may be diagnostically useful.[19-23] Recently, we reported that miRNA expression profiling is an effective and reliable tool for making the distinction between MM and reactive mesothelial cells in PE, complementary to cytologic evaluation.[6]

The objective of the current study was to assess the possible use of miRNAs as diagnostic markers to differentiate MM from lung AdC, especially in the challenging field of PE cytology.

MATERIALS AND METHODS

Materials

From the archives of the pathological anatomy department at the University of Padua (period of storage, 2010-2015), we retrieved the formalin-fixed and paraffin-embedded histologic samples of 41 pleural epithelioid MM cases and 40 lung AdC cases along with the cytological specimens of 26 pleural epithelioid MM cases and 27 lung AdC cases from PEs of a different cohort of patients. The age of the histologic and cytological samples was equally distributed. The clinicopathological features of the 2 series of patients are summarized in Table 1. Each cytological case had subsequent histologic confirmation. All cases were reviewed and the diagnoses were confirmed in all instances by 2 pathologists (A.F. and R.C.) according to the current World Health Organization classification.[3]

Microdissection, Total RNA Extraction, and Retrotranscription

Tumor cell enrichment was performed to ensure a tumor cell content >70%. To avoid cross-contamination, a new sterile microtome blade was used to cut 5 consecutive sections measuring 10 μm in thickness from each histologic sample. Tumor cells were microdissected manually from these sections with sterile needles under a light microscope and collected in 1.5-mL tubes. Total RNA was extracted using the RecoverAll Total Nucleic Acid Isolation Kit for formalin fixation and paraffin embedding (ThermoFisher Scientific, Waltham, Mass) following the manufacturer's instructions, as reported elsewhere,[24] and finally eluted in 50 μL of diethylpyrocarbonate (DEPC)-treated water.

With regard to the cytologic specimens, after coverslip removal, the cells were scraped from each slide with sterile razor blades and collected in 1.5-mL tubes. Total RNA was isolated using TRIzol Reagent (ThermoFisher Scientific) according to the manufacturer's protocol, as previously reported.[6] Total RNA finally was resuspended in 50 mL of DEPC-treated water.

The RNA concentrations of all the extractions were assessed using 1 μL of the sample and the Qubit RNA HS Assay Kit (ThermoFisher Scientific) on a Qubit 3.0

TABLE 1. Clinicopathological Characteristics of the 2 Series of Patients

Specimen	Diagnosis	No. of Cases	Mean Age ± SD, Years	Age Range, Years	Male/ Female
Histologic	MM	41	66.6 ± 4.7	56-82	30/11
	AdC	40	63.4 ± 5.1	47-83	24/16
Cytological	MM	26	73.2 ± 6.8	62-84	17/9
	AdC	27	65.3 ± 5.4	52-79	17/10

Abbreviations: AdC, adenocarcinoma of the lung; MM, malignant mesothelioma; SD, standard deviation.

TABLE 2. Primer Sequences of the Selected miRNAs and the Reference Gene Used For Quantitative Real-Time PCR

MiRNA	Primer Sequence
MiR-130a(-3p)	5′-CAGTGCAATGTTAAAAGGGCAT-3′
MiR-193a	5′-AACTGGCCTACAAAGTCCCAGT-3′
MiR-675	5′-TGTATGCCCTCACCGCTCA-3′
MiR-141	5′-GCTAACACTGTCTGGTAAAGATGG-3′
MiR-205	5′-CTTCATTCCACCGGAGTCTG-3′
MiR-375	5′-CGGCTCGCGTGAGGC-3′
RNU6B	5′-ACGCAAATTCGTGAAGCGTT-3′

Abbreviations: miRNA, microRNA; PCR, polymerase chain reaction.

Fluorometer (ThermoFisher Scientific) and stored at -80°C until further use.

Total RNA was retrotranscribed using the NCode VILO miRNA cDNA Synthesis Kit (ThermoFisher Scientific) following the manufacturer's instructions, as described elsewhere.[6] The complementary DNA obtained was stored at -80°C until further use.

Bioinformatic Analysis for miRNA Selection

Expression data of 1047 miRNAs and corresponding clinical information for lung AdC (511 cases) and MM (87 cases) data sets were downloaded from The Cancer Genome Atlas (TCGA) data portal in November 2015 (http://tcga-data.nci.nih.gov). The collection of the data from the TCGA platform was compliant with laws and regulations for the protection of human subjects and necessary ethical approvals were obtained. Two other data sets regarding the expression of 1111 miRNAs were collected and included 35 MM samples from GSE40345 and 25 lung AdC samples from GSE63805. All the data were log2-transformed. The normalization was performed using the quantiles normalization, as implemented in the Bioconductor "affy" package.[25] BRB-ArrayTools Data Archive-R/BioConductor (version 2.10) was used to perform the Student *t* test over the experiments of 2 classes.[26] All *P* values (<.05) were 2-sided.

Quantitative Polymerase Chain Reaction

Quantitative real-time polymerase chain reaction (qRT-PCR) was performed using the NCode EXPRESS SYBR GreenER miRNA qRT-PCR Kit (ThermoFisher Scientific) method according to the manufacturer's protocol, as previously reported.[6] The sequences of the primers of the 6 selected miRNAs and of the housekeeping small nuclear gene RNU6B are reported in Table 2. All reactions were performed in triplicate, including no-template controls, in a LightCycler 480 Real-Time PCR System (Roche, Mannheim, Germany). Relative quantification was calculated using the $2^{-\Delta\Delta Ct}$ method normalized to the expression of the internal reference gene RNU6B.

Statistical Analysis

Normality of the distribution of the miRNA expression data among the cases of MM and lung AdC was assessed by both graphical (box plot and Q-Q plot) and formal (Shapiro-Wilk test) methods. In the absence of normality, the Wilcoxon rank sum test with continuity correction was applied to detect significant differences in miRNA expression between the groups. In cytological specimens, the receiver operating characteristic (ROC) curve and the area under the ROC curve (AUC) were used to assess the ability of miRNA to differentiate between groups. The Youden test was applied to determine the best cutoff value along with the relative sensitivity, specificity, positive predictive value, negative predictive value, and accuracy of the miRNA. All the statistical analyses were performed with R statistical software (version 3.2.3; R Foundation for Statistical Computing, Wien, Austria). A *P* value <.05 was considered to be statistically significant.

RESULTS

Selected miRNAs

After the normalization, 239 of 1047 miRNAs included in the TCGA data sets (22.8%) were differentially expressed

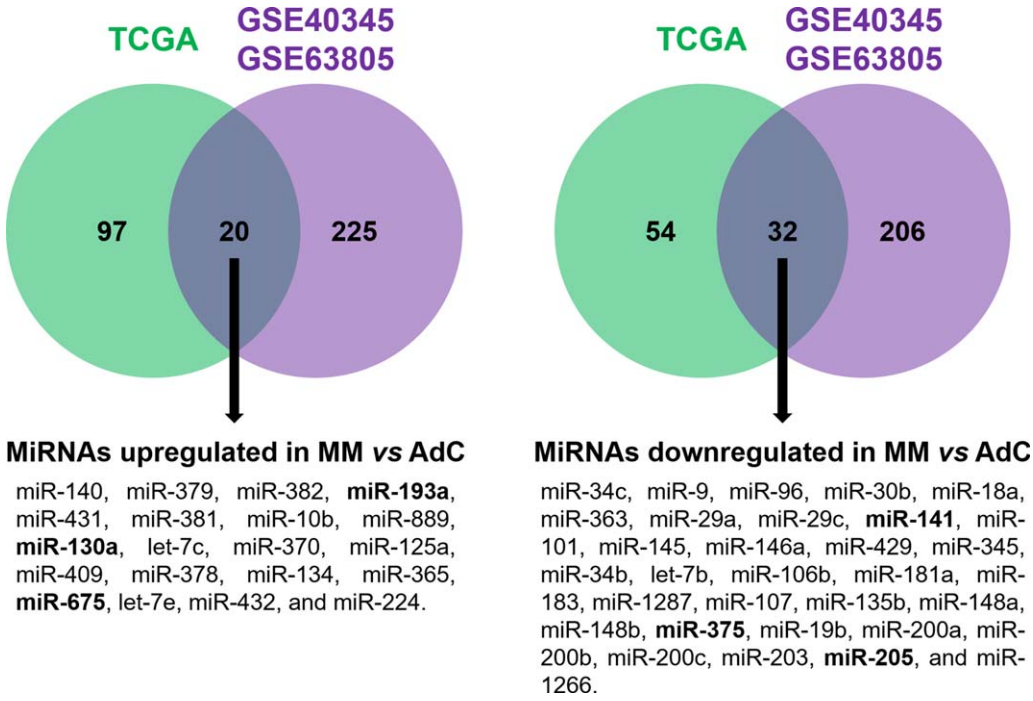

Figure 1. Chart showing the final step of the microRNA (miRNA) selection process from publicly available data sets. AdC indicates adenocarcinoma; MM, malignant mesothelioma; TCGA, The Cancer Genome Atlas.

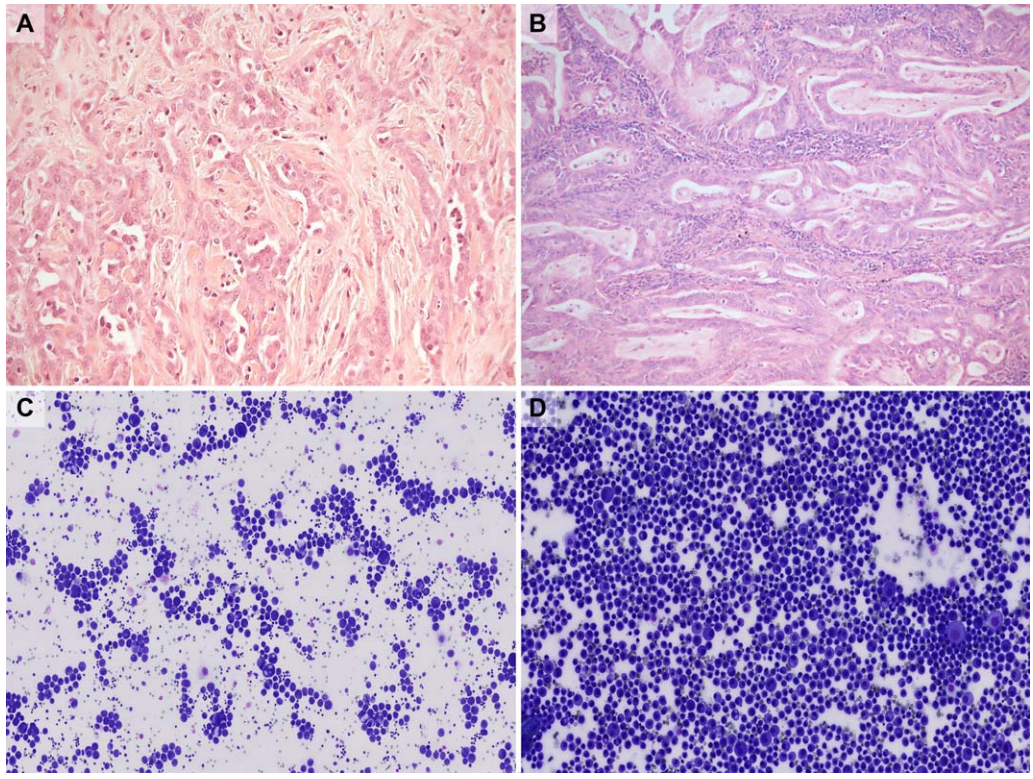

Figure 2. Representative photomicrographs of cases of (A and C) malignant mesothelioma and (B and D) lung adenocarcinoma from the histologic (A and B; H & E stain, original magnification ×200) and cytological (C and D; May-Grunwald-Giemsa stain, original magnification ×200) series of specimens.

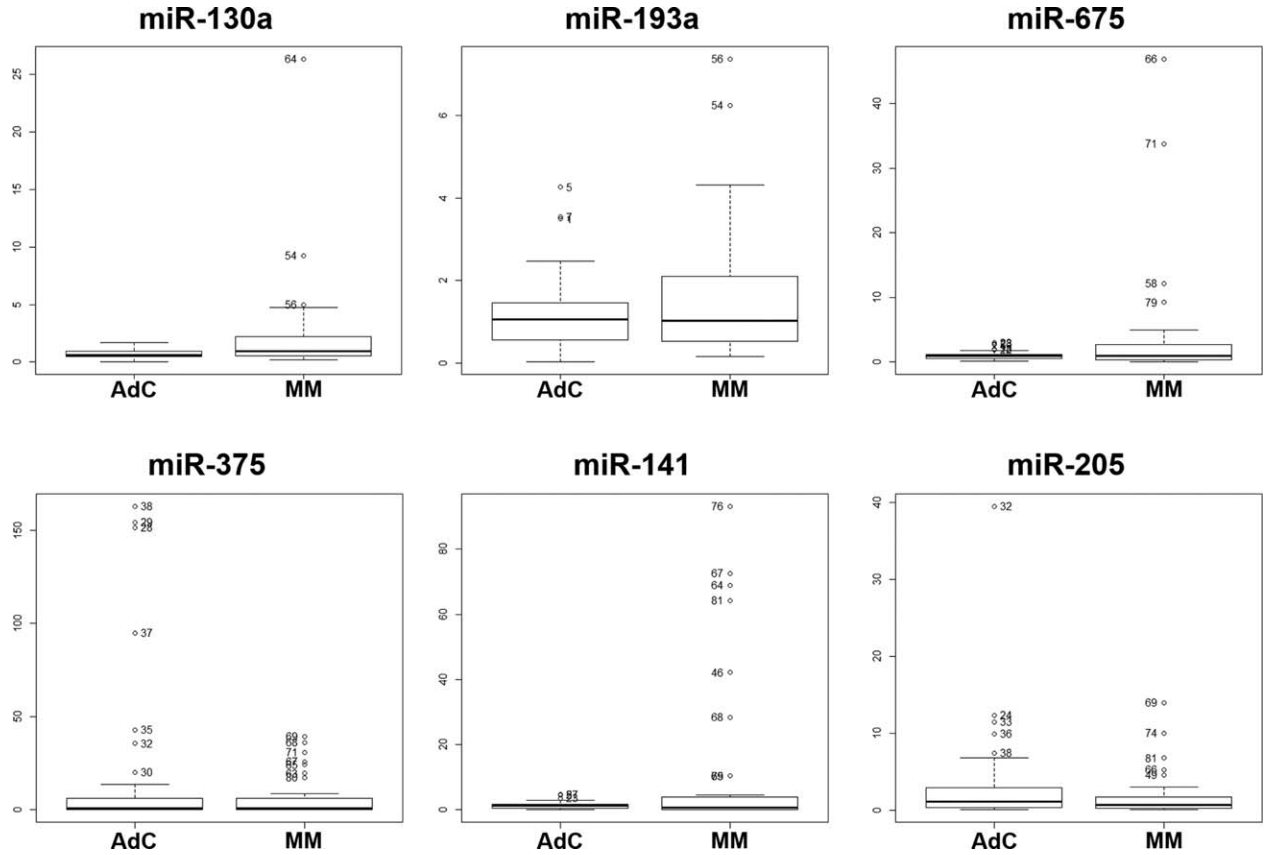

Figure 3. Box plots showing expression of the 6 microRNAs (miRNAs) selected from publicly available data sets in the histologic series of malignant mesotheliomas (MMs) and lung adenocarcinomas (AdCs). Only miR-130a was found to be significantly overexpressed in MM cases compared with lung AdC cases (P = .029).

with a fold change >1.5 in either direction from the miRNA median value between MM and lung AdC. Of these, 203 had a $P<.05$ and were included in the final comparison. The same analysis was performed on the data obtained from the other 2 independent platforms, and found 596 of 1111 miRNAs (53.6%) with a different expression. Of these, 483 had a $P<.05$ and were analyzed further. The list of the upregulated and downregulated miRNAs in both of the independent comparisons was used for the final selection of the candidates able to predict the nature of the tumor (Fig. 1). The selected miRNA panel comprised 3 upregulated miRNAs (miR-130a, miR-193a, and miR-675) and 3 downregulated miRNAs (miR-141, miR-205, and miR-375) in MM versus lung AdC. In particular, miR-675 demonstrated the highest fold-change among the most overexpressed miRNAs in the largest data set (TCGA) and miR-193a and miR-130a were among the top 15 upregulated miRNAs in both data sets, whereas miR-375 was by far the most downregulated in the TCGA data set, followed by miR-141 (selected also as representative of the miR-200 family, whose members all were among the top 15 downregulated miRNAs) and miR-205 (the only one of the top 15 downregulated miRNAs to be in both data sets).

Histologic Specimens

The expression levels of miR-130a, miR-193a, miR-675, miR-141, miR-205, and miR-375 were assessed in 41 epithelioid MM and 40 lung AdC histologic specimens (Fig. 2). The mean cycle threshold (Ct) values in the MM samples were 19.30 ± 2.30 for RNAU6B, 27.02 ± 2.83 for miR-130a, 28.81 ± 2.70 for miR-193a, 29.09 ± 2.12 for miR-675, 31.13 ± 4.26 for miR-141, 27.19 ± 3.36 for miR-205, and 27.25 ± 3.10 for miR-375, whereas in the AdC cases, the mean Ct values were 19.64 ± 1.14 for RNAU6B, 29.03 ± 3.23 for miR-130a, 30.60 ± 1.68 for miR-193a, 29.35 ± 1.10 for miR-675, 26.16 ± 1.17 for miR-141, 28.50 ± 2.25 for miR-205, and 29.77 ± 3.81 for miR-375. miR-130a was found to be remarkably upregulated (P = .029) in MM compared with lung AdC

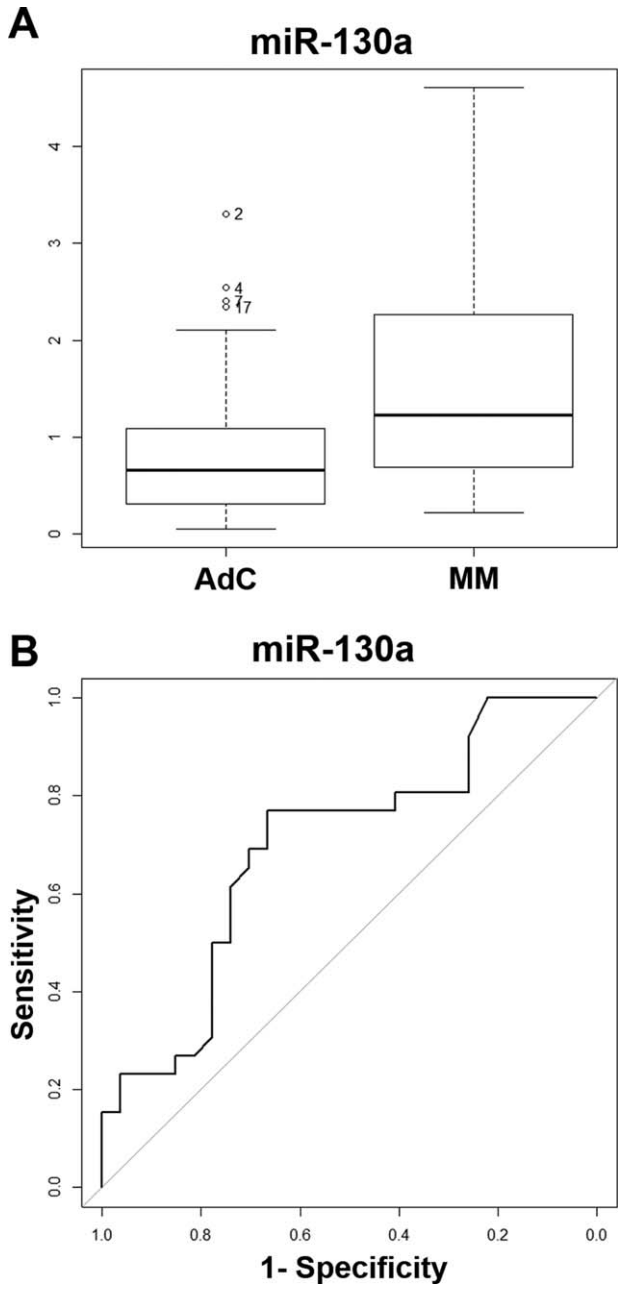

Figure 4. (A) Box plot showing expression of the microRNA 130a (miR-130a) in the cytological series of malignant mesotheliomas (MMs) and lung adenocarcinomas (AdCs). MiR-130a was found to be significantly overexpressed in MMs compared with lung AdC cases (P = .014). (B) Receiver operating characteristic (ROC) curve showing the diagnostic performance of miR-130a expression analysis in differentiating MM from lung AdC in pleural effusion specimens. The area under the ROC curve was 70% (95% confidence interval, 55%-84%), indicating moderate accuracy for miR-130a.

(Fig. 3). Although maintaining their respective upward and downward profiles of expression in MM versus lung AdC, miR-675 (P =.824) and miR-205 (P =.473) did not reach statistical significance (Fig. 3). The expression levels of miR-193a (P =.799), miR-141 (P =.175), and miR-375 (P =.992) were found to be similar between the 2 tumors (Fig. 3).

Cytological Specimens

All 6 miRNAs were quantified further in the cytological specimens of 26 epithelioid MM and 27 lung AdC (Fig. 2). The mean Ct values in the MM samples were 21.07 ± 2.40 for RNAU6B, 29.11 ± 2.57 for miR-130a, 30.07 ± 2.83 for miR-193a, 31.14 ± 2.02 for miR-675, 32.30 ± 3.76 for miR-141, 28.56 ± 3.26 for miR-205, and 29.15 ± 3.18 for miR-375, whereas the mean CT values in the lung AdC cases were 21.68 ± 1.77 for RNAU6B, 30.83 ± 2.90 for miR-130a, 32.20 ± 2.08 for miR-193a, 31.30 ± 1.88 for miR-675, 28.41 ± 2.03 for miR-141, 30.01 ± 2.40 for miR-205, and 31.37 ± 3.20 for miR-375. miR-130a demonstrated a significantly higher level of expression (P =.014) in MM compared with lung AdC (Fig. 4), in contrast to miR-193a (P =.841), miR-675 (P =.948), miR-141 (P =.356), miR-205 (P =.424), and miR-375 (P =.797). To determine the diagnostic power of miR-130a in PE cytology, the ROC curve was plotted from the qRT-PCR data (Fig. 4) and the AUC was calculated. The AUC was 70% (95% confidence interval, 55%-84%). Thus, miR-130a was moderately accurate in differentiating MM from lung AdC. The best cutoff value for the expression of miR-130a to discriminate between the 2 tumors was 0.675 (95% confidence interval, 0.5952-0.9231). This threshold enabled the correct identification of 20 of 26 MM cases and 18 of 27 lung AdC cases, demonstrating a sensitivity of 77%, a specificity of 67%, a positive predictive value of 69%, a negative predictive value of 75%, and an accuracy of 72%.

DISCUSSION

Complementary or alternative ancillary methods to IHC are necessary to differentiate epithelioid MM from lung AdC in histologic specimens and in PE samples. The current study tested miRNA expression profiling to address this issue. Bioinformatic analysis of the expression data of a significant number of miRNAs (1047 and 1111, respectively) from publicly available MM (87 and 35 cases, respectively) and lung AdC (511 and 25 cases, respectively) data sets provided a panel of 6 differentially expressed

miRNAs: miR-130a, miR-193a, miR-675, miR-141, miR-205, and miR-375. When tested by qPCR in the current series, only miR-130a was found to be concordant with the high-throughput results demonstrating significantly higher expression levels in MM compared with lung AdC. A possible explanation for this discrepancy may be the type of material analyzed. Both the TCGA and Xu et al[27] used only MM of pleural origin, as in the current study. However, among the 87 MM cases from TCGA, 57 were epithelioid, 23 were biphasic, 1 was sarcomatoid, and 6 were not otherwise specified. With regard to the GSE40345 data set, the case series comprised 18 epithelioid, 4 biphasic, and 3 sarcomatoid MM cases. On the contrary, only pure epithelioid MM cases were deliberately included in our histologic and cytological series because the sarcomatoid component rarely sheds cells in PE. It is likely that MM spindle cells harbor a different expression profile from epithelial-shaped cells, as also supported by our previous finding that miR-205 downregulation correlates with the sarcomatoid phenotype in MM.[1] Thus, the inclusion of all 3 MM subtypes due to MM rarity could have affected the current study results. Moreover, we performed manual microdissection of the histologic specimens to enrich the tumor cell content, whereas both Xu et al and Robles et al also might have analyzed a consistent amount of contaminant inflammatory or stromal cells.[27,28] Finally, technical aspects might have influenced the results of the current study because different next-generation sequencing platforms with diverse analytical performances were applied to build the various data sets.[27,28]

The findings of the current study demonstrated that miR-130a is significantly overexpressed in MM compared with lung AdC in both histologic and cytological samples and that it is moderately accurate in distinguishing the 2 tumors in PE specimens. This is in keeping with the data of Benjamin et al, in which miR-130a was found to demonstrate remarkably higher levels of expression in histologic specimens of MM (all subtypes) compared with those of a set of AdC samples of different origins.[29] However, in the current series, miR-130a quantification did not exceed the sensitivity or specificity threshold indicated by the IMIG for IHC markers (ie, 80%), reaching a value of 77% and 67%, respectively.[4] Thus, its diagnostic performances are similar but not superior to those of IHC; however, IHC is affected by several preanalytical (fixation and cut), analytical (antibody clones and staining conditions), and postanalytical (subjective interpretation) limitations. This accounts for the lack of an IMIG recommended panel of antibodies for MM diagnosis, and therefore each laboratory is responsible for developing its own panel. In addition, cases occur in which neoplastic cells do not stain with any marker. Instead, miRNA expression analysis has been demonstrated to be objective, able to be standardized, and feasible even in samples from archival stained/immunostained slides. Thus, it also can be performed as a second-level ancillary test in ambiguous or IHC-negative cases. The major limitation of its implementation in pathology laboratories is the availability of quantitative PCR systems. Indeed, contrary to IHC, this method is not available everywhere.

Similar to every other miRNA, miR-130a has hundreds of putative target genes and, in a given cancer, it can act as an oncogene or tumor suppressor gene depending on the specific target. However, with regard to MM, to the best of our knowledge no data currently are available regarding the role of miR-130a. Even though defining the function of miR-130a in MM is beyond the scope of the current study, we emphasize a possible intriguing link between this miRNA and the Hippo signaling pathway. This pathway controls organ size during embryonic development through inhibition of cell proliferation and the promotion of apoptosis, inactivating the transcription coactivator Yes-associated protein (YAP).[30,31] In cancer, defects in the pathway enable YAP to exert antiapoptotic, proproliferative, and stemness-promoting activities.[30,31] Several articles have reported modifications of the components of the Hippo signaling cascade in MM.[32-35] Recently, Shen et al reported a positive feedback loop involving YAP, miR-130a, and vestigial-like family member 4 (VGLL4): YAP directly induces miR-130a expression that represses VGLL4 expression, a YAP inhibitor, thereby unleashing and amplifying YAP oncogenetic activity.[36] Thus, the possible link between YAP and miR-130a in MM should be investigated.

The quantification of miR-130a expression could be a potential additional diagnostic tool with which to differentiate MM from lung AdC in PE cytology. Further validation in larger independent series of PE specimens is needed.

FUNDING SUPPORT

Stefano Volinia was supported by the Italian Association for Cancer Research (grants IG 13585 and IG 17063), the Ministry of University Education and Research (grant PRIN 2010), and EPIGEN for work performed as part of the current study.

CONFLICT OF INTEREST DISCLOSURES

The authors made no disclosures.

AUTHOR CONTRIBUTIONS

Rocco Cappellesso: Conceptualization, methodology, validation, formal analysis, writing–original draft, writing–review and editing, and visualization. **Marco Galasso**: Formal analysis and writing–original draft. **Lorenzo Nicolè**: Validation and investigation. **Paolo Dabrilli**: Investigation. **Stefano Volinia**: Formal analysis and resources. **Ambrogio Fassina**: Resources, supervision, project administration, and funding acquisition.

REFERENCES

1. Fassina A, Cappellesso R, Guzzardo V, et al. Epithelial-mesenchymal transition in malignant mesothelioma. *Mod Pathol.* 2012;25:86-99.
2. Peto J, Decarli A, La Vecchia C, Levi F, Negri E. The European mesothelioma epidemic. *Br J Cancer.* 1999;79:666-672.
3. Travis WD, Brambilla E, Burke AP, Marx A, Nicholson AG. WHO Classification of Tumours of the Lung, Pleura, Thymus and Heart. 4th ed. Lyon: International Agency for Research on Cancer; 2015.
4. Husain AN, Colby T, Ordonez N, et al; International Mesothelioma Interest Group. Guidelines for pathologic diagnosis of malignant mesothelioma: 2012 update of the consensus statement from the International Mesothelioma Interest Group. *Arch Pathol Lab Med.* 2013;137:647-667.
5. Cappellesso R, Millioni R, Arrigoni G, et al. Lumican is overexpressed in lung adenocarcinoma pleural effusions. *PLoS One.* 2015;10:e0126458.
6. Cappellesso R, Nicole L, Caroccia B, et al. Young investigator challenge: microRNA-21/microRNA-126 profiling as a novel tool for the diagnosis of malignant mesothelioma in pleural effusion cytology. *Cancer Cytopathol.* 2016;124:28-37.
7. Hjerpe A, Ascoli V, Bedrossian CW, et al; International Mesothelioma Interest Group; International Academy of Cytology. Guidelines for the cytopathologic diagnosis of epithelioid and mixed-type malignant mesothelioma: Complementary Statement from the International Mesothelioma Interest Group, Also Endorsed by the International Academy of Cytology and the Papanicolaou Society of Cytopathology. *Diagn Cytopathol.* 2015;43:563-576.
8. Kawamura K, Hiroshima K, Suzuki T, et al. CD90 is a diagnostic marker to differentiate between malignant pleural mesothelioma and lung carcinoma with immunohistochemistry. *Am J Clin Pathol.* 2013;140:544-549.
9. Comin CE, Dini S, Novelli L, Santi R, Asirelli G, Messerini L. h-Caldesmon, a useful positive marker in the diagnosis of pleural malignant mesothelioma, epithelioid type. *Am J Surg Pathol.* 2006;30:463-469.
10. Mimura T, Ito A, Sakuma T, et al. Novel marker D2-40, combined with calretinin, CEA, and TTF-1: an optimal set of immunodiagnostic markers for pleural mesothelioma. *Cancer.* 2007;109:933-938.
11. King JE, Thatcher N, Pickering CA, Hasleton PS. Sensitivity and specificity of immunohistochemical markers used in the diagnosis of epithelioid mesothelioma: a detailed systematic analysis using published data. *Histopathology.* 2006;48:223-232.
12. Ordonez NG. Application of immunohistochemistry in the diagnosis of epithelioid mesothelioma: a review and update. *Hum Pathol.* 2013;44:1-19.
13. Llinares K, Escande F, Aubert S, et al. Diagnostic value of MUC4 immunostaining in distinguishing epithelial mesothelioma and lung adenocarcinoma. *Mod Pathol.* 2004;17:150-157.
14. Jordon D, Jagirdar J, Kaneko M. Blood group antigens, Lewisx and Lewisy in the diagnostic discrimination of malignant mesothelioma versus adenocarcinoma. *Am J Pathol.* 1989;135:931-937.
15. Pai RK, West RB. MOC-31 exhibits superior reactivity compared with Ber-EP4 in invasive lobular and ductal carcinoma of the breast: a tissue microarray study. *Appl Immunohistochem Mol Morphol.* 2009;17:202-206.
16. Bishop JA, Sharma R, Illei PB. Napsin A and thyroid transcription factor-1 expression in carcinomas of the lung, breast, pancreas, colon, kidney, thyroid, and malignant mesothelioma. *Hum Pathol.* 2010;41:20-25.
17. Ohta Y, Sasaki Y, Saito M, et al. Claudin-4 as a marker for distinguishing malignant mesothelioma from lung carcinoma and serous adenocarcinoma. *Int J Surg Pathol.* 2013;21:493-501.
18. Garzon R, Calin GA, Croce CM. MicroRNAs in cancer. *Annu Rev Med.* 2009;60:167-179.
19. Fassina A, Cappellesso R, Fassan M. Classification of non-small cell lung carcinoma in transthoracic needle specimens using microRNA expression profiling. *Chest.* 2011;140:1305-1311.
20. Fassina A, Marino F, Siri M, et al. The miR-17-92 microRNA cluster: a novel diagnostic tool in large B-cell malignancies. *Lab Invest.* 2012;92:1574-1582.
21. Simonato F, Ventura L, Sartori N, et al. Detection of microRNAs in archival cytology urine smears. *PLoS One.* 2013;8:e57490.
22. Fassina A, Cappellesso R, Simonato F, et al. A 4-MicroRNA signature can discriminate primary lymphomas from anaplastic carcinomas in thyroid cytology smears. *Cancer Cytopathol.* 2014;122:274-281.
23. Cappellesso R, Tinazzi A, Giurici T, et al. Programmed cell death 4 and microRNA 21 inverse expression is maintained in cells and exosomes from ovarian serous carcinoma effusions. *Cancer Cytopathol.* 2014;122:685-693.
24. Barzon L, Cappellesso R, Peta E, et al. Profiling of expression of human papillomavirus-related cancer miRNAs in penile squamous cell carcinomas. *Am J Pathol.* 2014;184:3376-3383.
25. Bolstad BM, Irizarry RA, Astrand M, Speed TP. A comparison of normalization methods for high density oligonucleotide array data based on variance and bias. *Bioinformatics.* 2003;19:185-193.
26. Zhao Y, Simon R. BRB-ArrayTools Data Archive for human cancer gene expression: a unique and efficient data sharing resource. *Cancer Inform.* 2008;6:9-15.
27. Xu Y, Zheng M, Merritt RE, et al. miR-1 induces growth arrest and apoptosis in malignant mesothelioma. *Chest.* 2013;144:1632-1643.
28. Robles AI, Arai E, Mathe EA, et al. An integrated prognostic classifier for Stage I lung adenocarcinoma based on mRNA, microRNA, and DNA methylation biomarkers. *J Thorac Oncol.* 2015;10:1037-1048.
29. Benjamin H, Lebanony D, Rosenwald S, et al. A diagnostic assay based on microRNA expression accurately identifies malignant pleural mesothelioma. *J Mol Diagn.* 2010;12:771-779.
30. Piccolo S, Cordenonsi M, Dupont S. Molecular pathways: YAP and TAZ take center stage in organ growth and tumorigenesis. *Clin Cancer Res.* 2013;19:4925-4930.
31. Cappellesso R, Bellan A, Saraggi D, Salmaso R, Ventura L, Fassina A. YAP immunoreactivity is directly related to pilomatrixoma size and proliferation rate. *Arch Dermatol Res.* 2015;307:379-383.
32. Mizuno T, Murakami H, Fujii M, et al. YAP induces malignant mesothelioma cell proliferation by upregulating transcription of cell cycle-promoting genes. *Oncogene.* 2012;31:5117-5122.

33. Murakami H, Mizuno T, Taniguchi T, et al. LATS2 is a tumor suppressor gene of malignant mesothelioma. *Cancer Res.* 2011;71: 873-883.
34. Sekido Y. Inactivation of Merlin in malignant mesothelioma cells and the Hippo signaling cascade dysregulation. *Pathol Int.* 2011; 61:331-344.
35. Fujii M, Toyoda T, Nakanishi H, et al. TGF-β synergizes with defects in the Hippo pathway to stimulate human malignant mesothelioma growth. *J Exp Med.* 2012;209:479-494.
36. Shen S, Guo X, Yan H, et al. A miR-130a-YAP positive feedback loop promotes organ size and tumorigenesis. *Cell Res.* 2015;25: 997-1012.